BJES Basrah Journal for Engineering Sciences

Basrah Journal for Engineering Sciences, Vol. 25, No. 1, (2025), 47-55

Original Article

Journal homepage: www.bjes.edu.iq
ISSN (Online): 23118385, ISSN (Print): 18146120

The Impact of Iraqi Crude Oil Sulphur Content on the Mechanical Characteristics and Corrosion Resistance of Various Carbon Steel Grades Pipeline Welded Joints

Mohammed Yahya Lafth [1]*, Haider Mahdi Lieth [2]

[1,2] *Department of Mechanical Engineering, College of Engineering, University of Basrah, Basrah, Iraq*
E-mail addresses: pgs.mohammed.yahya@uobasrah.edu.iq, haider.lieth@uobasrah.edu.iq

Article Info

Article history:
Received: 11 January 2025
Revised: 27 January 2025
Accepted: 2 February 2025
Published: 16 August 2025

Keywords:
Sulphur content, Corrosion rate, API 5L, ASTM A106, Welded pipelines, Weight loss.

https://doi.org/10.33971/bjes.25.1.7

Abstract

The enormous volume of crude oil that needs to be transported results from the growing demand for petroleum. One of the most practical ways to move crude oil is via pipelines. This paper's primary objective is to examine the effects of sulphur, one of the components of crude oil, on welded pipes (API 5L X60, X46, and X42 pipes as well as ASTM A106 pipes). It also aims to show how sulphur content influences different kinds of pipes separately from the other important components of crude oil. The sulphur content of crude oil is determined using the TR-TCXRF equipment. The corrosion rates of welded pipes in four immersion solutions (Different percentages of sulphur content) were computed using weight loss. The samples' corrosion characteristics were assessed morphologically using an optical microscope (OM), scanning electron microscopy (SEM), and energy dispersive spectroscopy (EDS). Petroleum welded pipelines' mechanical qualities and resistance to corrosion are significantly impacted by sulphur; an increase in sulphur concentration resulted in a higher rate of corrosion and a decrease in mechanical properties. Among all the welded pipes utilized in the paper, the API 5L X60 welded pipe had the highest corrosion rate, whereas X46 welded pipe was more corrosion-resistant than X46 and X42 in API 5L-type pipes and ASTM A106 pipe.

1. Introduction

One of the most practical ways to move crude oil from producing locations to end users is via pipelines [1]. It was demonstrated that the most cost-effective and secure way to transport crude oils is through pipeline networks [2]. The formation of this piping system is impossible without the use of welding, which was a metallurgical operation [3]. Not only must the welding be robust, but the visual results must also fulfill requirements set by the Welding Procedure Specification (WPS) [4]. Both internal fluid pressure and severe external conditions must be tolerated by welded pipes [5]. Industrial pipes use carbon steel due to its accessibility, durability, and suitable mechanical characteristics [6]. The market value of crude oils can be ascertained by examining their physical characteristics, including density, dynamic viscosity, API gravity, and sulphur content [7]. The sulphur percentage (S%) of crude oil, which varies from less than 0.1% to more than 5%, is used to categorize it [8]. According to certain studies, sweet oil contains 0.5% sulphur, but sour oil has more than 0.5% sulphur. Environmental constraints necessitate those emissions from petroleum characteristics derived from these crude oils include low quantities of sulphur [9, 10].

Internal and exterior corrosion are the most common difficulties with pipelines used in oil and gas transmission [11]. It has been established that sulphur content in petroleum and its byproducts plays an important role in pipeline interior corrosion [12]. The rate at which the pipeline walls corrode depends on how aggressive the sulphur. Sulphur poses major security threats to crude oil transportation and causes problems with pipe systems [13]. The primary goal of this paper was to investigate the impact of different sulphur levels on the mechanical properties and corrosion resistance of API 5L (X42, X46, and X60) and ASTM A106 welded pipes. The microstructure and mechanical properties of carbon steel pipes are analyzed and compared. Weight loss is used to calculate the rate of corrosion of carbon steel welded pipes exposed to corrosive solutions (according to percentages of sulfur content).

2. Experimental work

2.1. Specimens preparation

In cooperation with Basra Oil Company, samples of API 5L (X42, X46, and X60) and carbon steel ASTM A106 were contracted following tensile and chemical testing to verify pipe quality prior to the completion of the remaining tests. Chemical analysis was performed in accordance with (ASTM A751-14, a) standard [14] using a spectrum analyzer apparatus (Model SPECTROTEST TXC25) depicted in Fig. 1 to determine the chemical composition of API 5L (X42, X46, and X60) and ASTM A106 pipes. The standard ranges (max. or min. to max.) for all elements explain the discrepancies in chemical composition between the actual test results and the standard values, and the tests that were obtained fell within the ranges, as indicated in Tabe1.

Table 1. Shows the weight percentage of the chemicals in API 5L (X42, X46, and X60) and ASTM A106 pipes.

X42	C	Mn	P		S	V	Nb	Ti
	Max.	*Max.*	*Min.*	*Max.*	*Max.*	*Max.*	*Max.*	*Max.*
Standard [15]	0.28	1.3	-	0.03	0.03	≤ 0.15%	≤ 0.15%	≤ 0.15%
Actual	0.226	0.55	0.003		0.002	0.004	0.011	0.002
X46	**C**	**Mn**	**P**		**S**	**V**	**Nb**	**Ti**
	Max.	*Max.*	*Min.*	*Max.*	*Max.*	*Max.*	*Max.*	*Max.*
Standard [15]	0.28	1.4	-	0.03	0.03	≤ 0.15%	≤ 0.15%	≤ 0.15%
Actual	0.225	0.54	0.003		0.0069	0.004	0.011	0.002
X60	**C**	**Mn**	**P**		**S**	**V**	**Nb**	**Ti**
	Max.	*Max.*	*Min.*	*Max.*	*Max.*	*Max.*	*Max.*	*Max.*
Standard [15]	0.28	1.4	-	0.03	0.03	≤ 0.15%	≤ 0.15%	≤ 0.15%
Actual	0.135	1.4	0.003		0.002	0.032	0.011	0.002
ASTM A106	**C**	**Mn**	**P**		**S**	**V**	**Nb**	**Cr**
	Max.	*Max.*	*Min.*	*Max.*	*Max.*	*Max.*	*Max.*	*Max.*
Standard [16]	0.3	1.06	-	0.035	0.035	0.08	0.15	0.4
Actual	0.281	0.43	0.003		0.002	0.004	0.011	0.055

Fig. 1 Mobile Spectro metal analysis.

The corrosion behavior of welded pipes was explored utilizing weight loss in crude oil samples with varying sulphur concentrations. The impact of sulphur percentages on welded pipeline corrosion was determined using an immersion process. Prior to the experiment, 16 specimens (pieces) were cut from API 5L (X42, X46, and X60) and ASTM A106 pipes using wire-cut machining with pieces dimensions (50 × 20 × 10) mm for API 5L X60 and ASTM A106, and (50 × 20 × 8.5) mm for API 5L (X46 and X42). Surface grinding was performed using a metallographic lapping machine that adhered to the ASTM E3 standard [17] and several grades of emery paper (120, 200, 400, 600, 800, 1000, 1200, and 2000). The 16 specimens were divided into four groups depending on their immersion media surroundings (four media).

2.2. Sulphur content analysis of crude oil

Determine the percentage of sulphur in the crude oil for the twelve samples from various Iraqi oil sites listed in Table 2 using the TR-TCXRF instrument depicted in Fig. 2. Out of the twelve samples, four were chosen based on the variation in the crude oil's sulphur content.

As indicated in Table 3, the four samples span the minimum to maximum reading range.

Table 2. Measurements of sulfur concentration from twelve sites in Iraq.

No. Sample	Location	Sulphur content (%)
1	Missan refinery	3.9436
2	Najaf refinery	3.9529
3	Nasiriya refinery	3.8839
4	Sayni refinery	3.411
5	Daura refinery	4.2533
6	Bazyan refinery	3.784
7	Baiji refinery	3.6844
8	Samaua refinery	4.4192
9	Kar refinery	3.644
10	Kassak refinery	3.8627
11	Basrah refinery	3.0399
12	Cayara refinery	5.7855

Fig. 2 TR-TCXRF (X-ray Fluorescence Sulphur Tester).

2.3. Prepared the hostile conditions.

Depending on the proportion of sulphur in the crude oil for the four samples in table 3. The four solutions were created to immerse the samples during the weight loss test. The concentration of sulphuric acid (H_2SO_4) was calculated, and it will be diluted with distilled water (4 liters) based on the sulphur percentage from the dilution equation below (equation 1) to produce the four solutions. Table 3 shows the four sulphuric acid solutions diluted in 4 liters of distilled water.

$$C_1 V_1 = C_2 V_2 \quad (1)$$

Where $C1$ is the concentration of the concentrated solution, $V1$ is the volume of the concentrated solution, $C2$ is the concentration of the diluted solution, $V2$ is the volume of the diluted solution, and S is a solution.

Depending on its application and concentration, a sulfuric acid (H_2SO_4) solution can have a range of effects. Strong acids, such as sulfuric acid, release H+ ions and drastically lower the mixture's pH when they almost completely dissociate in water. Some organic and inorganic substances can be oxidized by concentrated sulfuric acid, which is a strong oxidant. Extremely acidic circumstances brought on by low pH can impact the solution's chemical equilibrium [18].

Table 3. The four sulfuric acid solution concentrations (immersion media).

Sample No.	Location	Sulphur content (%)	Sulphuric acid diluted in (4 liters) of distilled water (ml)
1	Cayara refinery	5.7855	0.3930 (S_1)
2	Daura refinery	4.2533	0.2889 (S_4)
3	Bazyan refinery	3.784	0.2570 (S_3)
4	Basrah refinery	3.0399	0.2065 (S_2)

2.4. Preparation welded samples

The pipe samples utilized in this investigation were prepared using shield metal arc welding (SMAW). Where samples of welded joints are for the same steel grades. The specifications used in the welded were: Root: Bohler (6010) 2.5 mm as well as Hot, Filling, and Cap: ESAB (7018) 2.5 mm. The weld was in the V shape. The test specimens were ready for the immersion procedure once the welding was finished.

3. Results and discussion

3.1. Corrosion rates (weight loss)

The weight loss analysis was a common, dependable, and fast quantitative test method for measuring the corrosion rates. It compares the sample weights before and after corrosion [19]. The experiments began with the initial weight measurements of the welded specimens. The welded specimens were subsequently subjected to four conditions of sulphuric acid at various concentrations ml dissolved in 4 liters distilled water $S_1 = 0.3930$, $S_2 = 0.2065$, $S_3 = 0.2570$, and $S_4 = 0.2889$ for particular exposure times 7, 14, 21, and 28 days. After the initial exposure time 7 days, the specimens are removed for cleaning, drying, and reweighing. The specimens were subsequently reintroduced to the second exposure period 14 days, and the experiments were completed after 28 days of immersion. The welded specimens were meticulously rinsed with deionized water and then dried in a hot air stream in compliance with the ASTM G1-03 [19] standard. Every experiment was carried out at room temperature

The weight loss in grams was calculated as the difference in weight before and after the test, and the corrosion behavior was determined using the following equation (2) [20].

$$CR = \frac{K\,W}{A\,T\,D} \quad \text{mm/y} \quad (2)$$

Where CR was the corrosion rate in millimeters per year (mm/y), K was a constant (8.76×10^4), T was the exposure period in hours, A was the area in cm^2, W was the mass loss in grams, and D was the density in grams per cubic centimeter.

The mass differential resulting from corrosive phenomena with respect to the sample surface is defined in this section. Every specimen undergoing corrosion testing has a time-dependent change in mass. As the specimen immersion period grows, mass loss weights increase in all environments. Equation (2) allowed us to calculate the corrosion rate by weighing the undamaged sample material both before and after the corrosion process (removing the corrosion product from the specimen after immersion). The average weight loss and corrosion rate for ASTM A106 and API 5L (X60, X46, and X42) pipes are displayed in Table 4.

Because the concentration of sulphur content was lower in the S_2 environment than in the other environments, the weight losses for API 5L X60 pipe in the S_2 environment were the lowest value for corrosion rate for the welded specimens included in Table 4. The S_4 environment is superior to the S_3 environment, whereas the S_3 environment is superior to S_2. As immersion time increases, the largest are seen in the S1 environment (higher than S_2, S_3, and S_4).

This also holds for ASTM A106 welded pipe and API 5L (X46, X42) welded pipes. Table 4 showed similar results for all four pipes: the S_2 environment had the least amount of corrosion, the S_3 environment had more corrosion than S_2, the S_4 environment had more corrosion than S_3, and the S_1 environment had the most corrosion due to a higher sulphur content concentration than the other environments.

Even though API 5L X60 has slightly greater quantities of alloying elements such as manganese, chromium, and nickel, these elements improve corrosion resistance by increasing the steel's capacity to produce as table and protective oxide layers, but welding alters the material's microstructure, produces residual stress, and modifies surface properties, it has a substantial impact on API 5L pipes' ability to withstand corrosion. Grain growth or phase shifts brought on by high temperatures might modify the microstructure of the material. This could make it less resistant to corrosion. Uneven heating and cooling caused by welding leave the pipeline with residual strains. These pressures have the potential to speed up complete corrosion in the presence of a corrosion medium.

According to Table 4, the API 5L X60 welded pipe had the highest average corrosion rate value in S_1 over a 28-day period 0.0387 mm/y. This was followed by the A106 welded specimen 0.0378 mm/y, the API 5L X42 welded specimen 0.0294 mm/y, and the API 5L X46 welded specimen 0.0280 mm/y, also shown in Fig. 3. This suggests that the X46 welded pipe was more resistant to corrosion (lowest average corrosion rate value) than the X60 and X42 welded pipes in API 5L-type pipes and ASTMA106 pipes.

Table 4. the weight loss and rate of corrosion for ASTM A106 and API 5L (X42, X46, and X60) welded pipes.

Pipe	Media	Weights (g)					ΔW (g)	CR (mm/y)
		Original	After immersion					
			1 Week	2 Weeks	3 Weeks	4 Weeks		
X60 W	S_1	41.7991	41.786	41.7732	41.7565	41.7454	0.0537	0.0387
	S_2	41.2505	41.239	41.2275	41.2116	41.1994	0.0511	0.0345
	S3	41.7158	41.703	41.6914	41.6746	41.6641	0.0517	0.0368
	S_4	41.2232	41.210	41.1979	41.1811	41.1703	0.0529	0.0378
X46 W	S_1	68.7132	68.699	68.686	68.6731	68.6588	0.0544	0.0280
	S_2	69.3274	69.315	69.3023	69.2886	69.2772	0.0502	0.0262
	S_3	68.6677	68.655	68.6422	68.6286	68.6144	0.0533	0.0269
	S_4	69.3564	69.343	69.3301	69.3168	69.3027	0.0537	0.0273
X42 W	S_1	70.7369	70.723	70.7072	70.6934	70.6832	0.0537	0.0294
	S_2	71.4093	71.396	71.3812	71.3689	71.3579	0.0514	0.0276
	S_3	69.3383	69.325	69.3096	69.2959	69.2858	0.0525	0.0285
	S_4	70.5714	70.558	70.5425	70.5286	70.5183	0.0531	0.0288
A106 W	S_1	80.8525	80.836	80.8157	80.7991	80.7823	0.0702	0.0371
	S_2	80.089	80.075	80.0558	80.0371	80.0242	0.0648	0.0342
	S_3	79.1867	79.172	79.152	79.1344	79.1211	0.0656	0.0348
	S_4	79.0737	79.058	79.0378	79.0211	79.0052	0.0685	0.0363

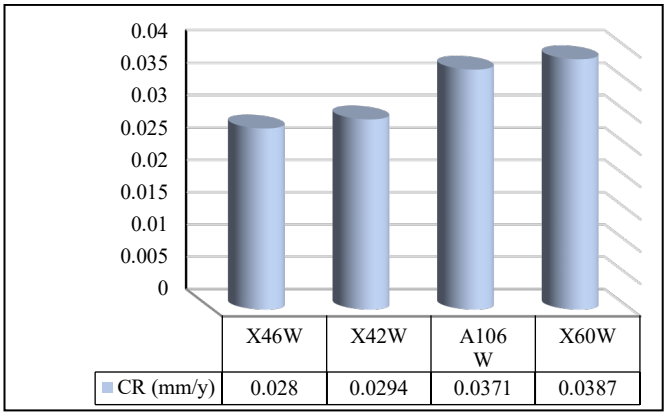

Fig. 3 Average rate of corrosion for four welded pipes in the S_1 medium.

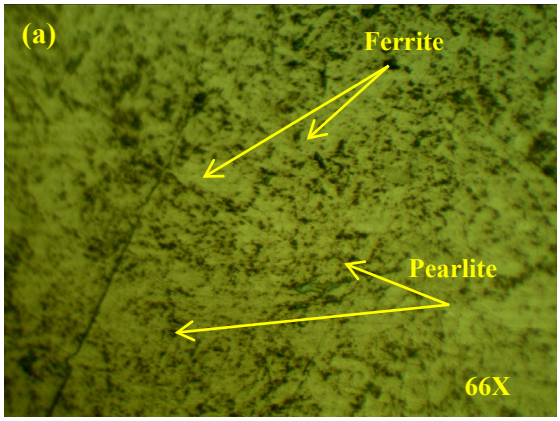

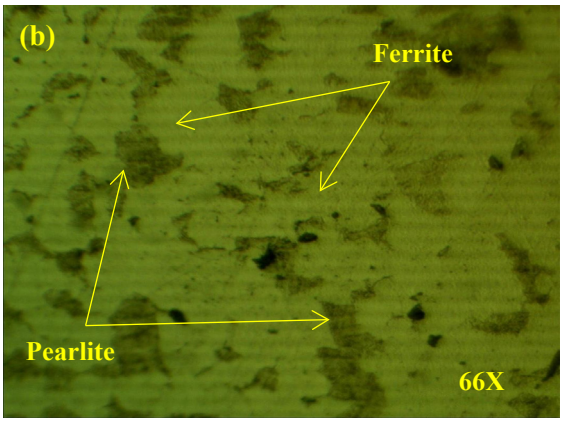

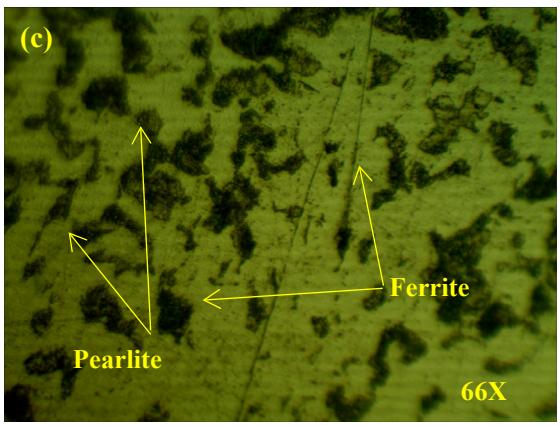

3.2. Microstructure analysis

Microstructure study was conducted using the OM and SEM machines. An optical microscope Type GX41 OLYMPUS from University of Basrah in the Mechanical Engineering department was used for the optical microscope (OM) research. On the other hand, the Alkhora Company conducted the tests in Baghdad using a SEM (INSPECT F-50) fitted with electron dispersive spectroscopy (EDS) in accordance with ASTM E 1508-12a [21].

The microstructures and variations in the polished surface of pipelines API 5L (X42, X46, X60) and ASTM A106 were revealed before the corrosion test using the optical microscope (OM) equipment shown in Fig. 4 and the (SEM) test shown in Fig. 5.

When examining the microstructure by (OM) with the etchant used was Nital solution, the phases that appear are largely ferrite with fine-grain pearlite for X60. Ferrite grains and pearlite colonies, which have a characteristic banded microstructure, create the microstructure of X46. Black flakes show that the X42 specimen exhibits pearlite banding in its structure, as well as visible ferrite grains containing pearlite. The ASTM A106 specimen has granules (bigger size than other pipes) of ferrite and pearlite.

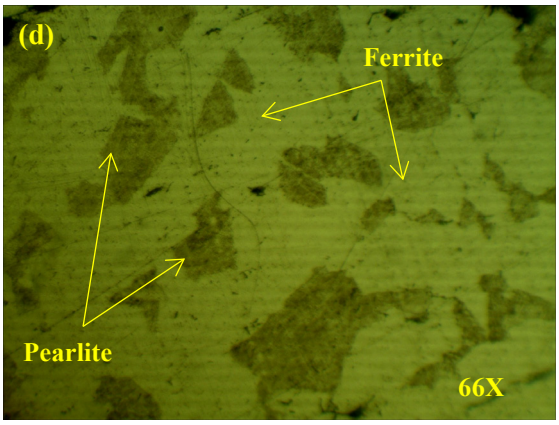

Fig. 4 OM images for pipes **(a)** X60, **(b)** X46, **(c)** X42, **(d)** ASTM A106 before corrosion (magnification was 66X).

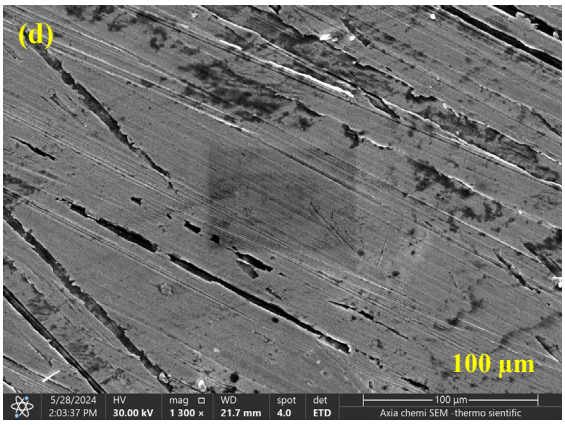

Fig. 5 SEM images for pipes **(a)** X60, **(b)** X46, **(c)** X42, **(d)** ASTM A106 before corrosion (magnification was 100 µm).

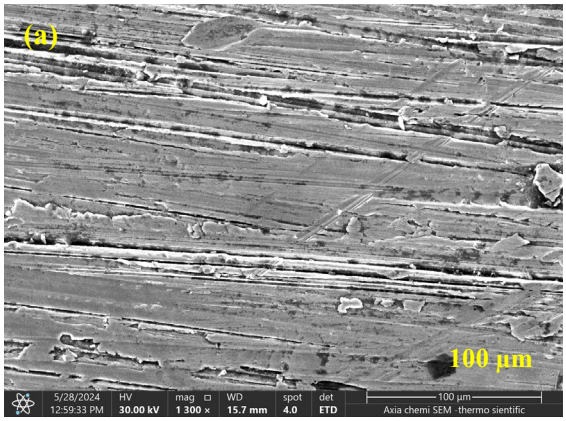

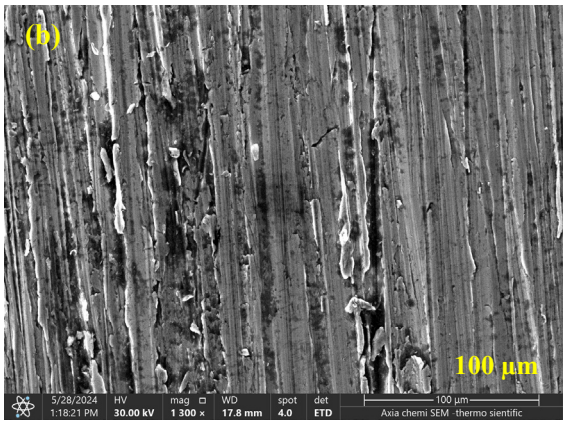

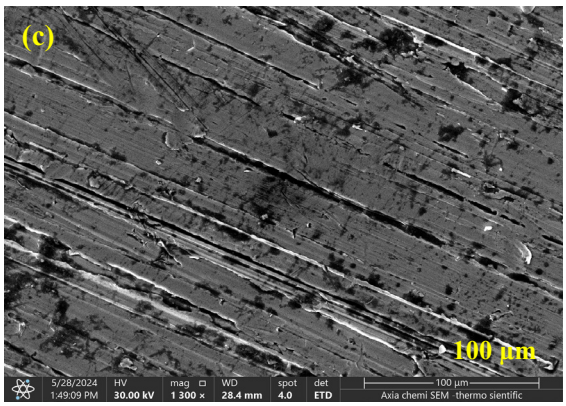

In settings with chlorides or other aggressive ions, sulfide inclusions can produce anodic sites in the steel microstructure, increasing the susceptibility to localized corrosion, including pitting and stress corrosion cracking. Excessive sulphur concentrations in API 5L steel usually result in undesired microstructural changes, such as the production of MnS inclusions and grain boundary segregation. The MnS inclusions are not directly apparent in optical or SEM images; nonetheless, their presence can be determined through electrochemical testing and corrosion behavior analysis. The relationship between the properties of MnS inclusions and pitting corrosion gives evidence for attributing corrosion processes to them [22, 23]. Still, sulphur in small levels can improve machinability. The performance of the steel in pipeline applications may be jeopardized by these alterations, which have a detrimental effect on the material's toughness, ductility, and corrosion resistance [24].

Figure 6 shows the micro-corrosion morphology of ASTM A106 welded pipelines and API 5L (X42, X46, and X60) welded pipelines within the immersion media following a 28-day immersion period. The SEM image demonstrates that the surface corrosion products of the four welded pipeline carbon steels were divided into two layers and that all carbon steel had uniform corrosion properties. The highest layer 10 µm of product corrosion was tough and irregularly distributed, whereas the bottom layer 100 µm was dense and had micro-cracks [25].

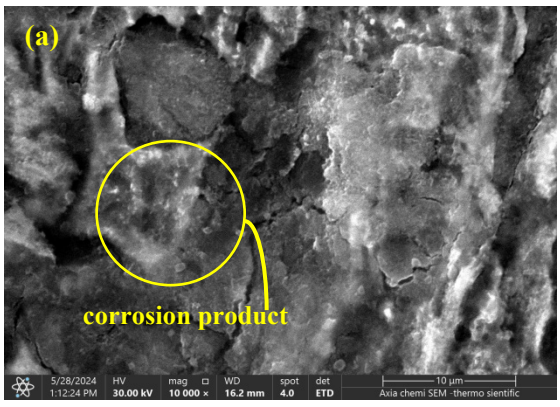

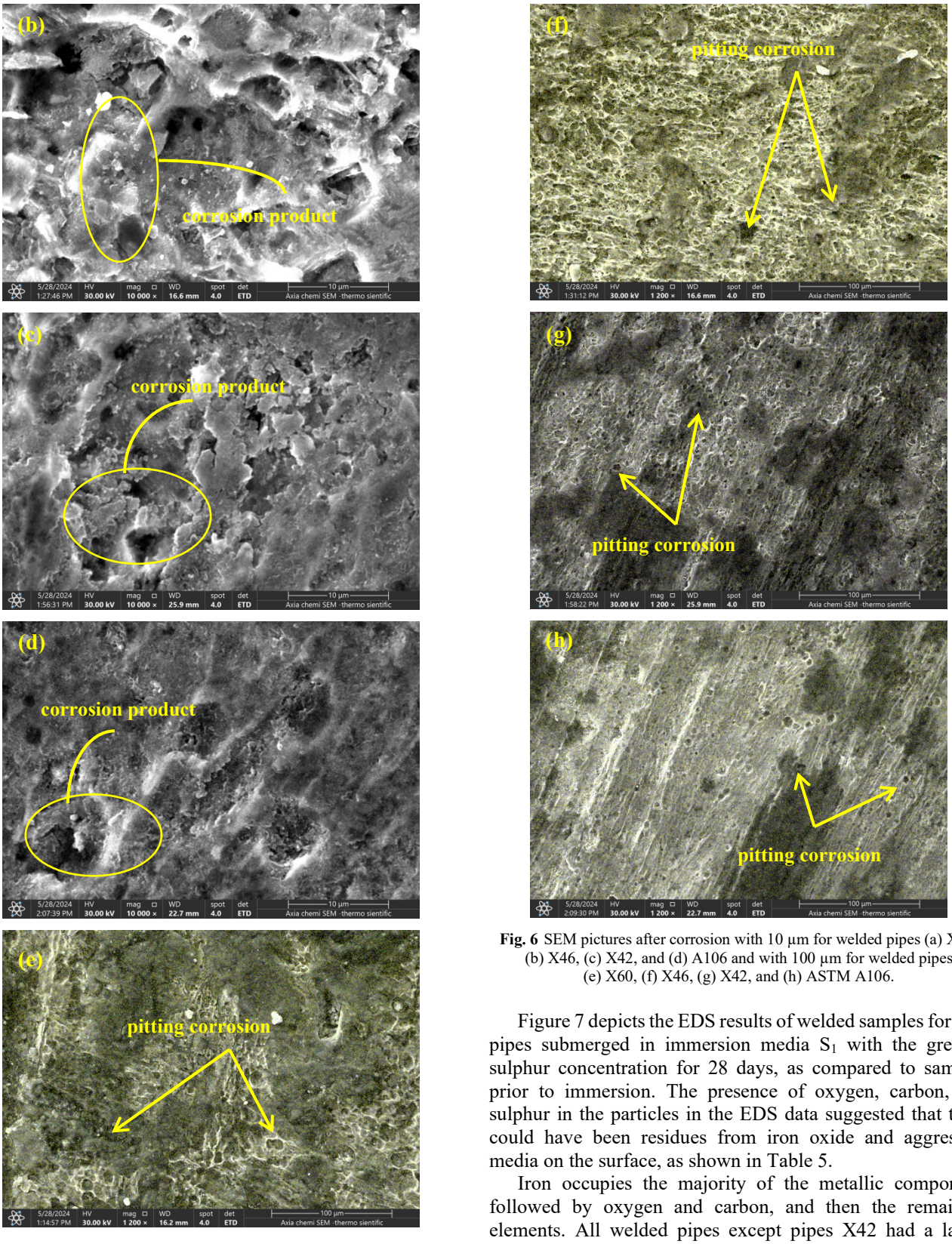

Fig. 6 SEM pictures after corrosion with 10 µm for welded pipes (a) X60, (b) X46, (c) X42, and (d) A106 and with 100 µm for welded pipes (e) X60, (f) X46, (g) X42, and (h) ASTM A106.

Figure 7 depicts the EDS results of welded samples for four pipes submerged in immersion media S_1 with the greatest sulphur concentration for 28 days, as compared to samples prior to immersion. The presence of oxygen, carbon, and sulphur in the particles in the EDS data suggested that there could have been residues from iron oxide and aggressive media on the surface, as shown in Table 5.

Iron occupies the majority of the metallic component, followed by oxygen and carbon, and then the remaining elements. All welded pipes except pipes X42 had a larger percentage of oxygen than carbon, and the sulphur percentage in X42 was higher than in all welded pipelines, as indicated in Table 5.

The EDS data indicated that iron sulfate Fe_2SO_4, iron sulfide FeS, and iron oxide Fe_2O_3 were among the corrosion products. The effect of sulfur content caused the above corrosion products compounds and accelerated corrosion (pitting) that lead to contributed to the degradation of the pipeline and the below corrosion equations illustrate the formation of these products.

$Fe + H_2SO_4 \longrightarrow FeSO_4 + H$

$Fe + S \longrightarrow FeS$

$4Fe + 3O_2 \longrightarrow 2Fe_2O_3$

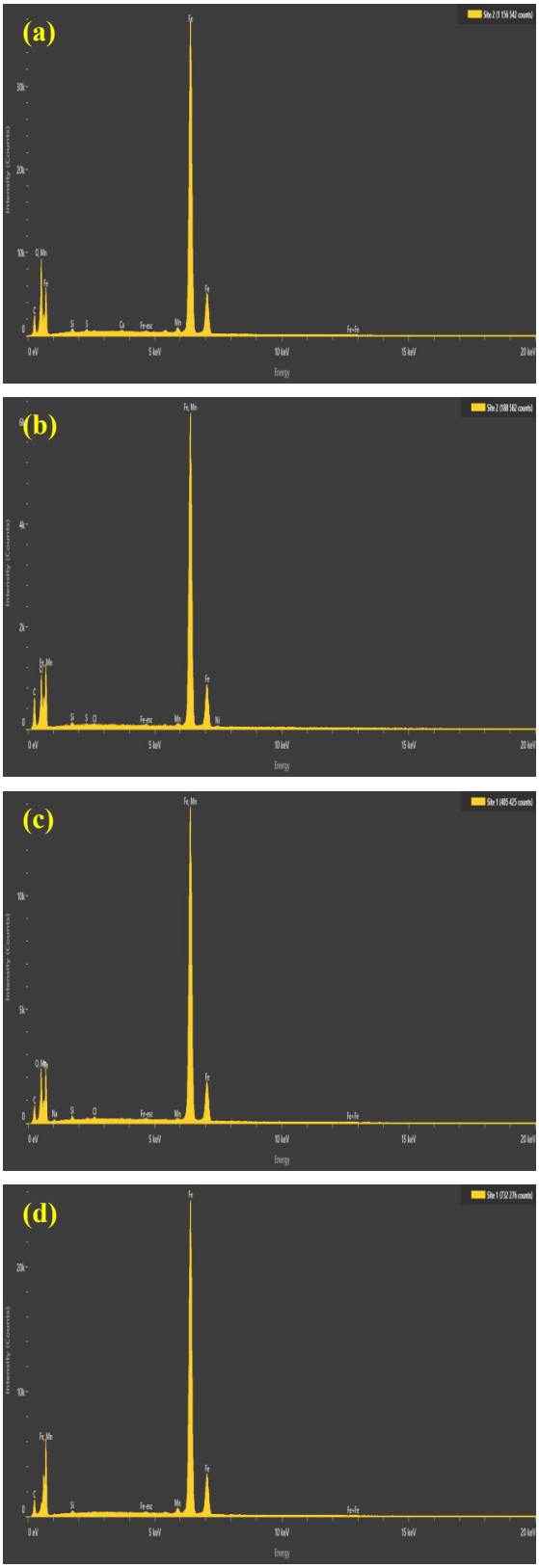

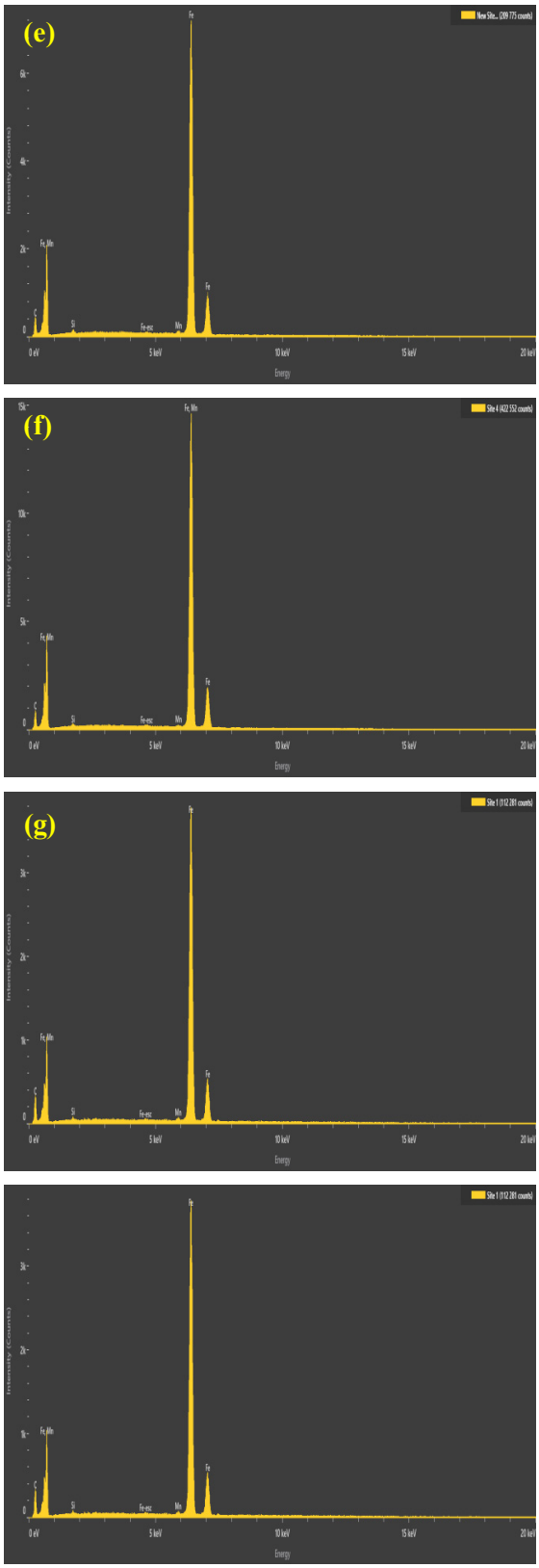

Fig. 7 EDS pictures for welded pipes before corrosion (a) X60, (b) X46, (c) X42, and (d) A106, and welded pipes after corrosion (e) X60, (f) X46, (g) X42, and (h) ASTM A106.

Table 5. EDS images for welded pipes before corrosion **(a)** X60, **(b)** X46, **(c)** X42, and **(d)** A106, and welded pipes after corrosion **(e)** X60, **(f)** X46, **(g)** X42 and **(h)** A106.

Pipe	Fe K		O K		C K		S K	
	Weight %	Atomic %	Weight %	Atomic %	Weight %	Atomic %	Weight %	Atomic %
X60W	72	41.4	17.6	35.4	8	21.5	0.1	0.1
X46W	78.9	49.5	10.4	22.9	8.8	25.7	0.1	0.1
X42W	75.1	43.5	10.4	21.1	12.3	33.1	0.2	0.2
A106W	75.8	45.6	12.6	26.4	9.2	25.8	0.1	0.1

4. Microhardness test

The Vickers Microhardness experiment was done on 20 specimens, 4 as received specimens and 16 from immersion test specimens and evaluated under ASTM E92 - 16 [26, 27] at room temperature with a load of 500 g and dwell of 15 s. The mean value was calculated by taking three readings from each specimen.

The microhardness values for the carbon steel pipes (X42, X46, X60, and ASTM A106) were computed right away after a 28-day immersion test. Figure 8 shows how the corrosion process affected the microhardness of carbon steel pipes that were welded. These figures clearly show that microhardness decreases with immersion when compared to between pipes. Table 6 shows how hardness values diminish in all corrosive mediums S_1, S_2, S_3, and S_4).

Figure 8 illustrates a variation and fluctuation up and down in the hardness measured values after immersion, which is normal due to the microstructural changes in the surface (corrosion) during the immersion process and changes in sulphur concentrations in the immersion media, even though the hardness values after immersion were generally lower than the values before immersion.

In welded samples, the hardness was greatest at S_4 and lowest at S_2 in X60 pipe; highest at S_3 and least at S_1 in X46 pipe; greatest at S_2 and lowest at S_3 in X42 pipe; and highest at S_3 and least at S_4 in ASTM A106 pipe.

Table 6. Microhardness for API 5L (X60, X46, X42), and ASTM A106 welded pipes before and after immersion.

Pipe	Average Microhardness (HV)				
	Before immersion	After immersion			
		S_1	S_2	S_3	S_4
X60W	199	182.666	178.666	191.333	197.66
X46W	213	178.333	187.66	199	182.33
X42W	218.333	184	189.666	179.333	187
A106W	197.666	183	191.333	195	176.66

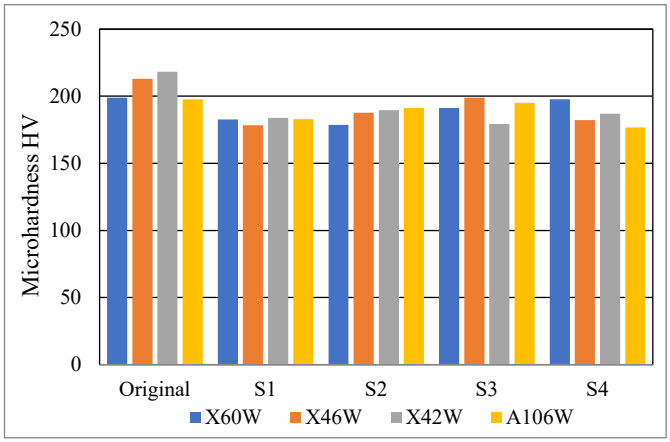

Fig. 8 Microhardness value changes for welded pipes (X42, X46, X60, and ASTM A106) before and after immersion.

5. Conclusions

Pipelines transport petroleum products, which are essential to the country's economy. This investigation confirmed that the corrosion phenomenon in the welded pipeline increased with increased sulphur concentrations in crude oil.

Used weight loss to calculate the corrosion rate of welded pipes API 5L (X42, X46, X60), and ASTM A106. The corrosion rate on welded pipeline surfaces increases with increasing H_2SO_4 concentration; specimens in S1 media with concentration 0.3930 exhibited the maximum corrosion rate 0.0387 mm/y for API 5L X60.

The corrosion rate of welded pipelines API 5L (X42, X46, X60) and ASTM A106 in the four immersion solutions (S_1, S_2, S_3, and S_4) rises with immersion time, as evidenced by weight loss findings. According to the EDS data, corrosion products included iron sulfate Fe_2SO_4, iron sulfide FeS, and iron oxide Fe_2O_3. The corrosion properties of the samples were evaluated morphologically.

The effect of sulphur content caused the above corrosion products these compounds accelerated corrosion (pitting) that leads to contributed to the degradation of the pipeline.

6. Recommendations

Other API 5L pipe types (including X80, X100, and X120) and additional elements found in crude oil, like salts and water, will be used as corrosive media in future studies.

References

[1] N. Narimani, B. Zarei, H. Pouraliakbar, and G. Khalaj, "Predictions of corrosion current density and potential by using chemical composition and corrosion cell characteristics in microalloyed pipeline steels," Measurement, Vol. 62, pp. 97-107, 2015. https://doi.org/10.1016/j.measurement.2014.11.011

[2] M. A. Adegboye, W. K. Fung, and A. Karnik, "Recent advances in pipeline monitoring and oil leakage detection technologies: Principles and approaches," Sensors, Vol. 19, Issue 11, 2019. https://doi.org/10.3390/s19112548

[3] T. N. Wordofa, and P. J. Ramulu, "Gas metal arc welding input parameters impacts on weld quality characteristics of steel materials a comprehensive exploration," Manufacturing Technology, Vol. 23, Issue 3, pp. 366-379, 2023. https://doi.org/10.21062/mft.2023.046

[4] P. Hargiyarto, K. Syauqi, S. Sugiyono, A. Ardian, S. Sianipar, and L. A. Nadjib, "Analysis of quality student practice results in shielded metal arc welding," Journal of Physics: Conference Series, Vol. 1700, Issue 1, 2020. https://doi.org/10.1088/1742-6596/1700/1/012010

[5] S. K. Sharma, S. Maheshwari, "A review on welding of high strength oil and gas pipeline steels," Journal of Natural Gas Science and Engineering, Vol. 38, pp. 203-217, 2017. https://doi.org/10.1016/j.jngse.2016.12.039

[6] H. M. Lieth, R. Al-Sabur, R. J. Jassim, and A. Alsahlani, "Enhancement of corrosion resistance and mechanical properties of API 5L X60 steel by heat treatments in different environments," Journal of Engineering Research, Vol. 9, Issue 4B, 2021. https://doi.org/10.36909/jer.14591

[7] Y. Liu, J. Zeng, S. Liu, and H. Long, "Physical properties variation of crude oil under natural laboratory and its geological implications: Dongying Sag, eastern China," Frontiers in Earth Science, Vol. 11, 2023. https://doi.org/10.3389/feart.2023.1169318

[8] S. M. Awadh, and H. S. Al-Mimar, "Statistical analysis of the relations between API, specific gravity and sulfur content in the universal crude oil," International Journal of Science and Research, Vol. 4, Issue 5, pp. 1279-1284, 2015.

[9] ASTM International, Standard Test Method for Sulfur in Petroleum Products by Wavelength Dispersive X-ray Fluorescence Spectrometry, ASTM International, 2010.

[10] A. K. Alzarqani, and F. J. Alduhaidahawi, "A Study of Sulfur Content in Crude Oil, Gasoline and Kerosene in Some Iraqi Oil Fields and Refineries," International Journal of Health Sciences, Vol. 6, Issue S4, pp. 10548-10557, 2022. https://doi.org/10.53730/ijhs.v6nS4.12233

[11] F. O. Kolawole, S. K. Kolawole, J. O. Agunsoye, J. A. Adebisi, S. A. Bello, and S. B. Hassan, "Mitigation of Corrosion Problems in API 5L Steel Pipeline – A Review," Journal of Materials and Environmental Sciences, Vol. 9, Issue 8, pp. 2397-2410, 2018.

[12] P. C. Okonkwo, M. H. Sliem, R. A. Shakoor, A. M. A. Mohamed, and A. M. Abdullah, "Effect of temperature on the corrosion behavior of API X120 pipeline steel in H_2S environment," Journal of Materials Engineering and Performance, Vol. 26, pp. 3775-3783, 2017. https://doi.org/10.1007/s11665-017-2834-0

[13] M. Meriem-Benziane, B. Bou-Saïd, and N. Boudouani, "The effect of crude oil in the pipeline corrosion by the naphthenic acid and the sulfur: A numerical approach," Journal of Petroleum Science and Engineering, Vol. 158, pp. 672-679, 2017. https://doi.org/10.1016/j.petrol.2017.08.073

[14] ASTM A751-14. Standard Test Methods, Practices and Terminology for Chemical Analysis of Steel Products, 2014.

[15] I. S. Bott, F. Siciliano, G. Z. Batista, and J. M. Gray, "Line Pipe Steels," In Handbook of Pipeline Engineering, Cham: Springer International Publishing, pp. 285-310, 2024.

[16] ASTM International, Standard specification for seamless carbon steel pipe for high-temperature service, ASTM A 106, ASTM International, 2019.

[17] ASTM, E. Standard guide for preparation of metallographic specimens. American Society for Testing and Materials, West Conshohocken, 2011.

[18] A. H. Hattab, S. Beebany, A. S. Kaki, "The effect of H_2SO_4 concentration on corrosion of Kirkuk's oil and gas pipelines with studying corrosion reaction rates kinetically," Chemical Methodologies, Vol. 7, Issue 4, pp. 257-267, 2023. https://doi.org/10.22034/chemm.2023.376042.1632

[19] ASTM Committee G-1 on Corrosion of Metals, Standard practice for preparing, cleaning, and evaluating corrosion test specimens, ASTM international, 2017.

[20] ASTM Standard, Standard practice for laboratory immersion corrosion testing of metals, American Society for Testing and Materials G31-72, 2004.

[21] ASTM E1508-12a, Standard Guide for Quantitative Analysis by Energy-Dispersive Spectroscopy, 2012.

[22] S. Yang, M. Zhao, J. Feng, J. Li, C. Liu, "Induced-pitting behaviors of MnS inclusions in steel," High Temperature Materials and Processes, Vol. 37, Issue 9-10, pp. 1007-1016, 2018. https://doi.org/10.1515/htmp-2017-0155

[23] W. Shi, S. Yang, A. Dong, J. Li, "Understanding the corrosion mechanism of spring steel induced by MnS inclusions with different sizes," The Journal of the Minerals (Jom), Vol. 70, pp. 2513-2522, 2018. https://doi.org/10.1007/s11837-018-3026-6

[24] M. Nnoka, T. A. Jack, J. Szpunar, "Effects of different microstructural parameters on the corrosion and cracking resistance of pipeline steels: A review," Engineering Failure Analysis, Vol. 159, 2024. https://doi.org/10.1016/j.engfailanal.2024.108065

[25] Z. Wang, Z. Zhou, W. Xu, L. Yang, B. Zhang, Y. Li, "Study on inner corrosion behavior of high strength product oil pipelines," Engineering Failure Analysis, Vol. 115, 2020. https://doi.org/10.1016/j.engfailanal.2020.104659

[26] ASTM Standard, Standard Test Methods for Vickers Hardness and Knoop Hardness of Metallic Materials, Designation: E92-16, 2016.

[27] H. M. Lieth, M. A. Jabbar, R. J. Jassim, R. Al-Sabur, "Optimize the corrosion behavior of AISI 204Cu stainless steel in different environments under previous cold working and welding," Metallurgical Research and Technology, Vol. 120, Issue 4, 2023. https://doi.org/10.1051/metal/2023058